Data Efficient and Stability Indicated Sampling for Developing Reactive Machine Learning Potential to Achieve Ultra-long Simulation in Lithium Metal Batteries

Longkun Xu,* Wei Shao, Haishun Jin, and Qiang Wang*

Samsung Research China – Beijing (SRC-B), Beijing, 100102, China

E-mail: longkun1.xu@samsung.com; qiang.w@samsung.com

Abstract

Modelling the formation of solid-liquid interphase (SEI) is challenging as its strict requirement with both simulation accuracy and length. Machine learning potential (MLP) based molecular dynamics (MD) simulation is expected to play a role in this field while currently its use is hindered by sampling efficiency and simulation stability. In this work, we tackle the two challenges together. We propose the *stability-indicated-sampling* (SIS) algorithm for efficiently sampling training data using physical information (temperature). Unlike previous strategies, our method does not need prior knowledge of reaction networks or training multiple MLPs for uncertainty estimation. Compared with the recent proposed methods HAIR and DP-GEN, our approach gives significant improvement of sampling efficiency with less requirements with the initial training data, to realize $>$ 10 ns MLPMD simulation using *ab initio* MD (AIMD) trajectory of just a few ps. We introduce the concept *underlying instability consistency* by showing the accuracy of reaction mechanisms and radial distribution function

(RDF) can be improved by SIS-MLPMD, although their information is not explicitly used in our sampling decision. Furthermore, we show that long-time MLPMD simulation of Lithium metal battery (LMB) can not only reproduce some well-known SEI components including LiF, Li_2O, LiOH, LiS and the incomplete N-S breaking in high-concentration systems, but also ionic aggregation structures of LiF, which is not shown in our AIMD training data but matches previous results of electrochemical impedance spectroscopy. Our work is expected to help accelerate future investigations, especially for studying long-time ($\geq$ ns scale) reaction dynamics in interfacial problems.

1. Introduction

Understanding electrode-electrolyte interface and associated interface engineering is at the heart of modern battery chemistry.[1–3] The structure and components of SEI affects many crucial aspects of batteries including safety, duration, energy density and costs.[4] Electrolyte engineering is a crucial strategy to tune SEI and to develop advanced batteries through designing electrolyte concentration, structure and other aspects.[5–8] For example, it was reported that the concentration of electrolyte solution strongly affect the components and structures of SEI in LMB.[5,6,8] By tuning Li-O/F network, the number and positions of electron-withdrawing groups (EWG), Yu and co-workers made rational design of solvent molecules in electrolyte solution to reach an excellent performance with multiple properties including solvation and Coulombic efficiency.[7]

Simulating battery molecules and materials with physics-based and data-driven approaches enables high-throughput screening and design of battery electrolyte engineering, while it needs accurate and low-scaling interatomic potential to investigate the dynamics of related systems. In details, an accurate description of the fundamental electron-transfer (ET) and redox process requires modelling electrons with *ab initio* methods such as density functional theory (DFT) or post Hartree-Fock (HF) methods.[9] However, key process in battery systems (e.g., the formation of SEI) usually needs long-time simulation which hinders the use of

these *ab initio* methods, which makes the development and choice of simulation methods a challenge.[10] Among different low-scaling methods such as ReaxFF[11] and GFN-XTB,[12] machine learning potential (MLP) is one of the most active areas in recent years. In a nutshell, MLP leverages neural network based deep learning architecture or Gaussian approximation potential (GAP) to fit parameters to reproduce (or approach) the accurate energies and forces labelled with *ab initio* methods. Thus it is expected to transfer knowledge learnt from short-time simulation of small-scale systems to long-time simulation of large-scale systems.[13] MLP has made a diverse range of battery applications, to name just a few here. Jiao and co-workers employed deep potential molecular dynamics (DPMD)[14] to study the homogeneous deposition and surface self-healing of Lithium metal.[15] Batzner and co-workers developed NequIP, an E(3)-equivariant neural network approach, which efficiently gives accurate predictions on force, energy, radial distribution function (RDF) and diffusivity of $Li_4P_2O_7$, a promising solid electrolyte for LMB.[16]

Despite the great success of MLP in batteries, a large part of research has not been performed yet. First, currently available works mainly focus on the properties of either bulk electrode materials[15] or bulk electrolyte solution,[16,17] while the main bottleneck for battery simulation is actually modelling *interfaces* and SEI.[2] Using MLP for interfaces modelling is challenging, one reason is that the studied systems are much more complicated than that in the bulk phase, which introduces higher requirements for interfaces.[18,19] Another challenge is that interfaces usually hold complex interactions between different species, e.g., long-range interactions,[2,20] many-body interactions[21] and field effects,[22,23] which calls for higher accuracy of MLP.

Second, to the best of our knowledge, although have been employed for studying fundamental properties in electrochemistry (e.g., redox potential[17]) and reactions in other domains,[24,25] current MLP methods have not been used for modelling bond-breaking and bond-forming reactions of Li-salts at battery interface, because the complexity in reaction networks of SEI formation cannot be handled by a simple design of collective variables,[26] although

these reactions are essential to understand the formation of SEI and the complex reaction network in batteries. Developing reactive interatomic potential is notoriously difficult as it usually needs extra efforts with *sampling* strategies (e.g., enhanced sampling methods).[24,25] The recent work of Zhang and co-workers demonstrated massive computational resources are required to develop reactive MLP even for just simple CHON species.[27] Battery systems, as a contrast, often contains much more elements beyond CHON such as Li, F, P, S, Co, Ni, Mn, Fe and others. Another strategy to solve the sampling issue is active learning (AL), an extensive introduction about adaptive subsampling with active learning can be found in the recent work of Wen and co-workers.[28] However, the use of AL based sampling strategies often require uncertainty estimation using an ensemble of MLPs, which brings large computational costs.[29–31] Additionally, AL-based sampling requires a high diversity of the initial training data and data augmentation strategies.[32]

Last but not the least, the *stability* issues associated with MLP based molecular dynamics (MD) simulations has been discussed recently. For example, Fu and co-workers benchmarked several state-of-the-art (SOTA) MLP models for organic molecules and materials and found none of these models can generate stable simulations for all systems.[33] A more important information from this work is that simulation instability is an indicator for sampling insufficiency.[33] More strikingly, the recent work of Wu and Li showed stability is an issue with many SOTA MLPs even for the dynamics of one single simple organic molecule $C_7O_2H_{10}$.[34] Interestingly, although stability issue gains attention for MLP applications for small organic molecules, it has rarely reported for battery interface systems, which is much more complicated and is expected to meet more severe stability issues.

This work aims to address some of above-mentioned knowledge gaps and our contributions are summarized as follows:

(1) We present the first study (simulation length $>$ 10 ns) using MLP to model reactions of SEI formation in LMB. We highlight some crucial while previously uncovered factors in dealing with cut-off radius R_{cut}, using bulk configurations of electrodes and electrolyte

solution, and fixing atoms in slab model.

(2) We propose the SIS-MLPMD algorithm (see Figure 1) for efficiently sampling training data leveraging instability of physical information (temperature). Our method does not need prior knowledge of the reaction network or training an ensemble of MLPs for uncertainty measurement. It shows superior performance regarding efficiency and accuracy compared with other methods.

(3) We demonstrate the *underlying instability consistency* across different MLPs and properties, which justifies using only temperature instability information itself alone is sufficient to guide sampling.

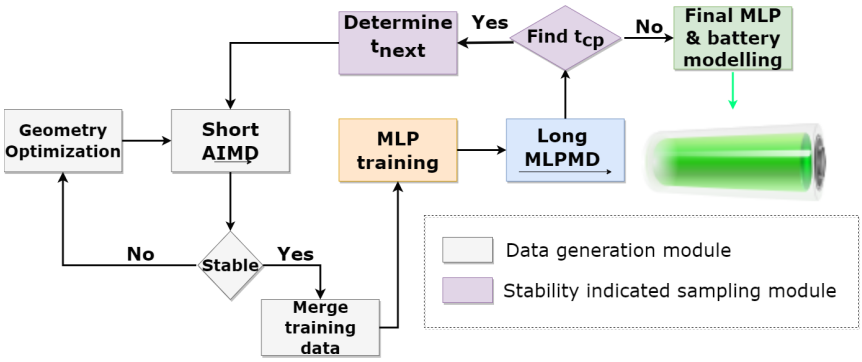

(a)

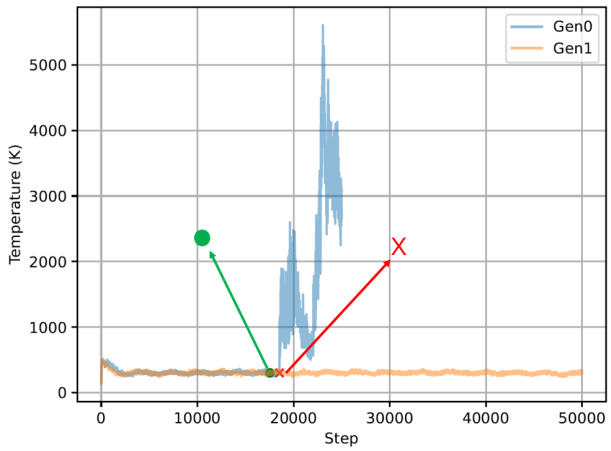

(b)

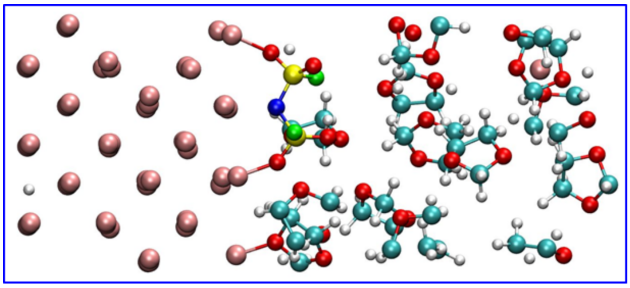

(c)

Figure 1: Scheme of our (a) SIS-MLPMD workflow (b) temperature stability indicated sampling and (c) 1M interface model. Pink, red, yellow, blue, green, cyan and white spheres in (c) respectively represents Li, O, S, N, F, C and H atoms. In (a), the input (structure, energy and force data) are obtained with a short *ab initio* molecular dynamics (AIMD) simulation without or with geometry optimization. In each generation, a long MLPMD is conducted with the trained MLP to find the temperature catastrophic point (t_{cp}, red cross in (b)) and associated starting point t_{next} (green dot in (b)) for next generation. The new training data is merged into that in the previous generation and the MLP model is fine-tuned with tunable learning rate and energy/force weight in the loss function. The iterations ends when a long and stable MLPMD output is obtained without any t_{cp}. Based on the final MLP, properties and reactions of the Li|LiFSI/DOL battery system are studied. See details in Note S1-S2.

2. Methods

2.1. Generating training data

Three systems are studied in this work, namely Li electrode, lithium bis(fluorosulfonyl)imide (LiFSI) in 1,3 dioxalane (DOL) electrolytes in different concentrations, and the interface between Li slab and LiFSI/DOL (see Figure 1c). All training data of energies and forces are labelled with *ab initio* MD (AIMD) simulation using CP2K (version 7.1).[35] AIMD labelled data are converted to `deepmd/npy` format using the `dpdata` tool in DeepMD-kit (version 2.1.1).[36] See more details in Note S1.

2.2. Training and test of MLP

Unless otherwise noted, all DPMD training in this work uses following procedure. All DFT data are shuffled and splitted into 60% training data, 20% validation data, and 20% test data. `se_e2_a` descriptor is used.

As discussed above and elsewhere,[33,34] stability is one of the major bottlenecks for current MLPMD simulation and the root of poor stability is usually the poor quality (e.g., data imbalance and data sparsity) of training data.[33] Although sampling strategies based on AL (e.g., DP-GEN[14]) have made great success, they often require training an ensemble of multiple MLPs, or the so-called *query by committee* method,[31] which brings extra computational costs in training multiple MLPs. As a contrast, herein we leverage instability issue itself as an indicator for sampling and consequently propose a sampling method SIS-MLPMD, see Figure 1. The idea in designing this algorithm is simple: once the MLP meets MD instability issue in one region $\mathcal{R}$ of sampling space, the probability of lacking training data in $\mathcal{R}$ is 100% (see relevant discussions in Ref.[33]), so in a nutshell, we don't use the uncertainty of model accuracy (that used in AL strategies) but the certainty of model inaccuracy (instability) to guide sampling.

In details, we start the SIS-MLPMD workflow by building the initial training data $\mathcal{D}_0$

and training the initial MLP model $\mathcal{M}_0$ with training data labelled with a short 2.5 ps AIMD simulation. Then we run a long MLPMD at target temperature T (default 300 K). If the temperature T_i at time t_i (i is the iteration number of SIS-MLPMD) is smaller than T_L or greater than T_H, we label the point t_i as the catastrophic point (t^i_{cp}). Then we run another short AIMD starting from t^i_{next} before t^i_{cp}, see details in Figure1b and Note S2.

T_L and T_H can be tunable on-the-fly with a coarse-to-fine strategy, i.e., in the first a few generations of SIS-MLPMD, $[T_L, T_H]$ can be a large range (e.g., [0K, 1000K]) to include many off-equilibrium structures and enable fast evolution of the MLP model to cover the expected time length (e.g., 1 ns), which we call *low-fidelity model*. While at the last a few generations, the temperature range is set as a small one (e.g., [200K, 500K]) to guarantee the quality of the final MLP model, which we call *high-fidelity model*. If the AIMD simulation from t^i_{next} is unstable or slow, this indicates the structure at t^i_{next} is too unphysical to get a converged wavefunction or a stable MD simulation, then the structure at t^i_{next} is optimized using PBE-D3/DZVP-MOLOPT-GTH in CP2K, before running the AIMD simulation.[35]

After getting the new training data $\mathcal{D}_i$, we merge the old training data $\mathcal{D}_{i-1}$ with $\mathcal{D}_i$ and obtain the new MLP model $\mathcal{M}_i$ while the initial learning rate is decreased accordingly to implement the mechanism of *learning without forgetting*,[37] which is crucial while often ignored in the field of MLP simulation. See more relevant details in Note S2.

2.3. MLPMD

All MLPMD in this work are run with LAMMPS (version 29 Oct 2020).[38] We run an energy minimization before NVT simulation, stopping tolerance for energy and force is respectively 1.0e-4 and 1.0e-6. The coordinates of the system are saved every 1 ps for further analysis.

3. Results and Discussion

3.1. Bond breaking sequence of LiFSI

The comprehensive reaction mechanism regarding with the degradation of Li salt on metal electrodes and associated formation of SEI remains a topic under debate.[5] One of the most crucial questions in this field concerns the bond breaking sequence of Li slat, and how it is affected by the concentration and solvation structure of electrolyte solution.[39–41] Specifically with bond breaking sequence, one question remains unclear is whether N-S bond or S-F bond of LiFSI breaks first in forming SEI. Our AIMD simulation obtained with CP2K supports the previous conclusion reported by Liu and co-workers,[5] i.e., we found F-S bond breaks at around 0.26 ps of the reaction, while N-S bond breaks at around 0.28 ps. A scheme visualizing system change through the reaction can be found in Note S3.

3.2. Overlooked effects of R_{cut}, bulk configurations, and fixing atoms

One reason why MLP has not yet been widely used in modelling reactions at battery interface is that many factors can affect the modelling accuracy as the system complexity is much higher than that of bulk electrode[15] and bulk electrolyte,[17] while there lacks a comprehensive study available to showcase the protocol. Here we raise three questions for crucial factors in battery modelling, namely the choice of suitable cut-off radius (R_{cut}), the correct use of bulk configurations of Li electrode and electrolyte solution, and the effects of freezing atoms in slab models.

R_{cut} is widely recognized as an important hyper-parameter determining the accuracy of trained MLP models, both in Behler-Parinello neural network (BPNN) based and graph neural network (GNN) based MLPs. It is also widely believed that the accuracy of trained MLP model would be necessarily benefited when increasing R_{cut}.[32,42] Here we challenge this opinion and our question is Q1: *Does larger cut-off radius always guarantee higher accuracy?*

There lacks a uniform agreement concerning whether or not to use bulk configurations

in the training set for modelling interfaces. For example, in the work of Eckhoff and Behler, bulk $Li_xMn_2O_4$ and water structures are used in the training data in studying $Li_xMn_2O_4$-water interface,[19] while in some other interface works bulk configurations were not used.[43] Wu and co-workers recently proposed ModDP strategy which builds training data for two end points along a reaction with DP-GEN, then refining the training data of intermediate states using random configurations.[44] The philosophy is actually pretty similar with using bulk configurations in the interface, see Fig.S6. So our question is Q2: *Is it helpful to use bulk configurations in the training set for studying interfaces?*

Freezing a few bottom layers of solid is one regular strategy in studying solid-liquid interfaces with slab models,[45,46] however it remains unclear whether this strategy is reasonable in generating training data for MLP, as artificial zero force is usually applied when freezing atoms, however DFT labelled forces is the main training data for MLP. Thus, the same element (e.g., Li) with the same chemical environment could have distinctly different reference values of force in DFT calculations, which could make the training data inaccurate. Our question is Q3: *Should atoms of Li slab be fixed or not in generating training data?*

To answer these questions, we conducted simulations for three systems: 1M and 4M bulk LiFSI/DOL electrolyte solution, and 1M Li|LiFSI/DOL interface, the tested *Rcut* values starts from 6 Å, which is a value frequently used in related works,[32,42,47] to up to 20 Å. All the answers to these questions are obtained by comparing test force RMSE of trained model. The main results can be seen in Figure 2, more details with hyper-parameters effects can be found in Note S4. Before discussing specific conclusions, a general observation in Figure 2 and Note S4 suggests our test RMSE of force and energy of all systems are respectively in the range of [0.06, 0.17] $eV/\AA$ and [1.63e-03, 9e-04] eV. Though small force and energy RMSEs are not sufficient to conclude the good quality of trained MLP,[33,34] we think they are the minimum requirements for a good MLP model. The accuracy is comparable with other battery-related MLP works in recent years,[16,17,32,48] which suggests our protocol to train MLP is reliable. Next, we discuss conclusions to the above three questions one-by-one.

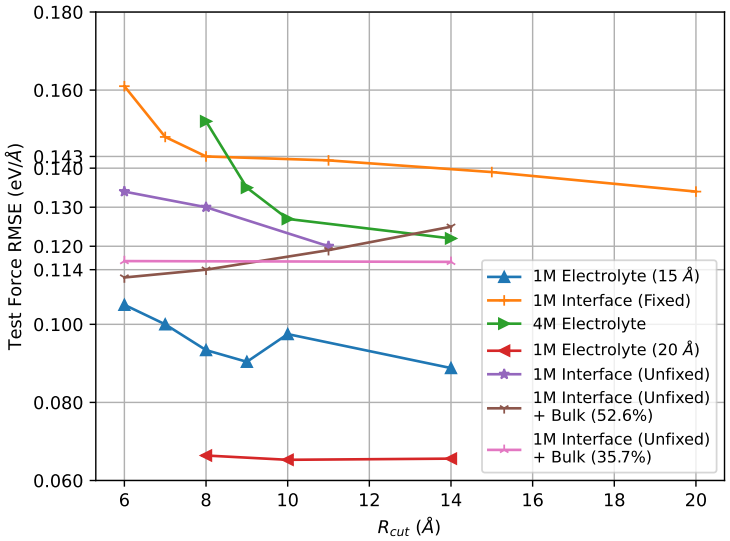

(a)

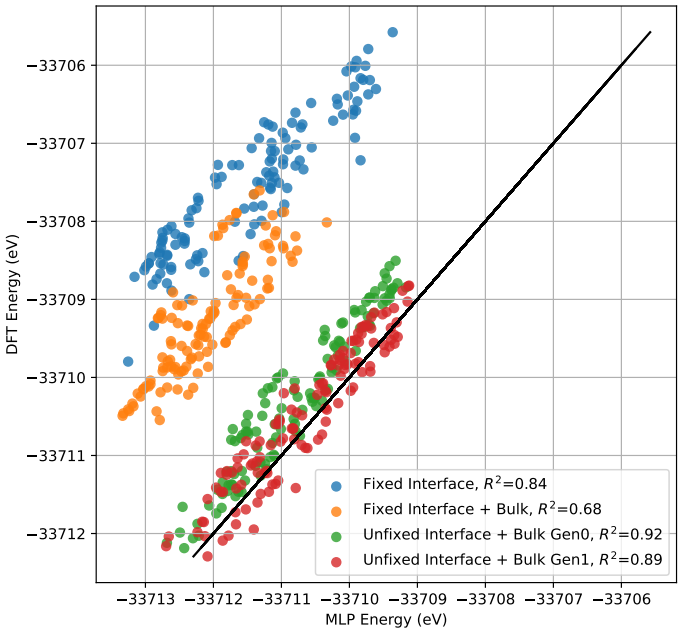

(b)

Figure 2: (a) Effects of studied factors on test force RMSE of trained MLPs. *1M* and *4M* respectively means the concentration of electrolyte solution, *15 Å* and *20 Å* respectively represents the size of unit cell. *Bulk* indicates using bulk configurations. *Fixed* and *Unfixed* respectively denotes whether atoms of Li slab are fixed in generating training data. 52.6% and 35.7% are the ratio of bulk configurations in the training set. Default options are: 1M, 15 Å, no bulk configurations, unfixed. (b) Parity plot between predicted MLP energies and DFT energies for 1M interface, using $R_{cut}6$. Note the training data size is the same for fixed and unfixed interface.

For Q1, our answer is that larger R_{cut} does not always guarantee higher accuracy, especially for low-concentration electrolyte solution (see $R_{cut}10$ in *1M Electrolyte (15 Å)* in Figure 2a and Tab.S4), and the conclusion is not affected by tuning various hyper-parameters (see Tab.S5-Tab.S9). A closer analyze of the results suggests that the position of *jump point* is related with the size of unit cells, it locates around $(2 \times (d/2)^2)^{1/2}$ where d is the length of unit cell (see Fig.S4-S5).

For Q2, we found it is crucial to use bulk configurations in modelling battery interface (see the difference between *Fixed Interface* and *Fixed Interface + Bulk* in Figure 2b). Without using bulk configurations of Li electrode and electrolyte solution, the predicted energies are systematically underestimated compared with DFT reference, and this error is almost unchanged by the increase of R_{cut}, see Fig.S7. Besides, our experiments with MACE[49] show the same trend, which further solid the conclusion that the observed systematically underestimation of predicted energies is independent on the choice of MLP models, but the missing of bulk configurations. To validate our assumption, we add bulk configurations of Li slab and electrolyte solution into the training data. Consequently for $R_{cut}8$, force improvement is around 12.3% (see Figure 2a, from 0.130 to 0.114 eV/Å). See details in Note S4-2.

For Q3, we found freezing atoms does lead to artificial zero force in the training data. After freeing the fixed atoms, the predicted energies and forces can be further improved, see Figure 2b. At $R_{cut}8$, force improvement is around 9.1% after unfixing atoms (see Figure 2a, from 0.143 to 0.130 eV/Å). To the best of our knowledge, our work is the first one highlighting the errors introduced by fixing atoms, which raises our concerns over whether slab model should be used in generating MLP training data. This matters not only for battery applications but also for other important chemistry problems at interfaces, e.g., electrocatalysis.[50,51] See details in Note S4-2.

Besides answering above three important questions, another interesting observation is that once bulk configurations are used, the RMSE of predicted energies and forces are nearly

independent on R_{cut} values. Using the smallest R_{cut} value can even give the best result, which we call *R_{cut}6 performs best* (see Note S4-3), and the result is not affected by tuning hyper-parameters, see Tab.S12-S14. This observation is out of our expectation as it seems widely recognized that interface systems require larger R_{cut} values for including long-range interactions.[2] However this result further validates our previous conclusion *larger R_{cut} does not guarantee higher accuracy*. As this phenomenon only appears when we use bulk configurations (see brown and purple lines in Figure 2a), we suspect a possible reason is that using bulk configurations and using larger R_{cut} values can both address long-range interactions, while using both strategies together can lead to double counting effects. To prove our assumption, we conducted a simple experiment by decreasing the ratio of bulk configurations in the training set, see results in Tab.S15, which concludes that *R_{cut}6 performs best* indeed is from the double-counting effects (see brown and pink lines in Figure 2a), and this observation keeps true for 10 M interface (see Tab.S16). The finding is useful as MLP training time is significantly affected by R_{cut}, and our results suggest that using a small R_{cut} value with bulk configurations might be the most accurate and economic way to modelling interfaces. As high-concentration battery interface is a crucial topic for current battery research,[52–54] this finding will be very valuable for future MLP works about batteries.

Our experiments with 1M interface using R_{cut}6 and R_{cut}11 suggests the choice of R_{cut} values not only affect MLP accuracy, but also the evolution of MLP for long-time simulations. With R_{cut}6, our MLP prediction with forces is pretty satisfied after only two iterations of SIS-MLPMD (see *Gen1* in Figure 2b) while the tests with R_{cut}11 is much worse after the same number of iterations (see *Gen1* in Fig.S8). As a result, our SIS-MLPMD can reach $>$ 1 ns simulation (see details below) after only 3 iterations with R_{cut}6, while with R_{cut}11, the SIS-MLPMD cannot reach 1 ns simulation after 7 iterations.

In summary, above three crucial yet easily overlooked factors, worth to be carefully treatment in future studies.

3.3. Comparison with HAIR and DP-GEN

After figuring out the roles of above factors, next we compare the performance of our SIS-MLPMD model with others. Here we choose HAIR[5] and DP-GEN[29] as HAIR represents one of the most advanced multi-scale physics methods to simulate long-time reactions. While DP-GEN represents one of the most sophisticated sampling strategies in MLP related research.[17,48]

Here we compare their performance with our method regarding both model accuracy and sampling efficiency, using 1M electrolyte solution as the test case. For sampling efficiency, we define a metric, acceleration ratio (AR), which measures the ratio of time-length of the whole trajectory and that of AIMD. HAIR method uses a fixed AR as 11 (i.e., a 0.5 ps AIMD followed by each 5 ps ReaxFF-MD, $11 = (0.5 + 5)/0.5$, see Ref.[5]). While our method gives AR as > 57 (i.e., 17.5 ps AIMD used to get 1 ns MLPMD simulation). The temperature of our MLPMD simulation is stable around our target 300 K except for the first a few steps of energy minimization, see Figure 3a. Note also our MLPMD time length could be much longer than 1 ns (see examples for 1 M and 10 M interface later) and thus AR could be much larger than 57. Nevertheless, it is clear that our AR is already over 5 times of that in HAIR, which means our method can realize long-time (> 1 ns) simulation using much smaller number of DFT data ($< 20\%$ of that in HAIR).

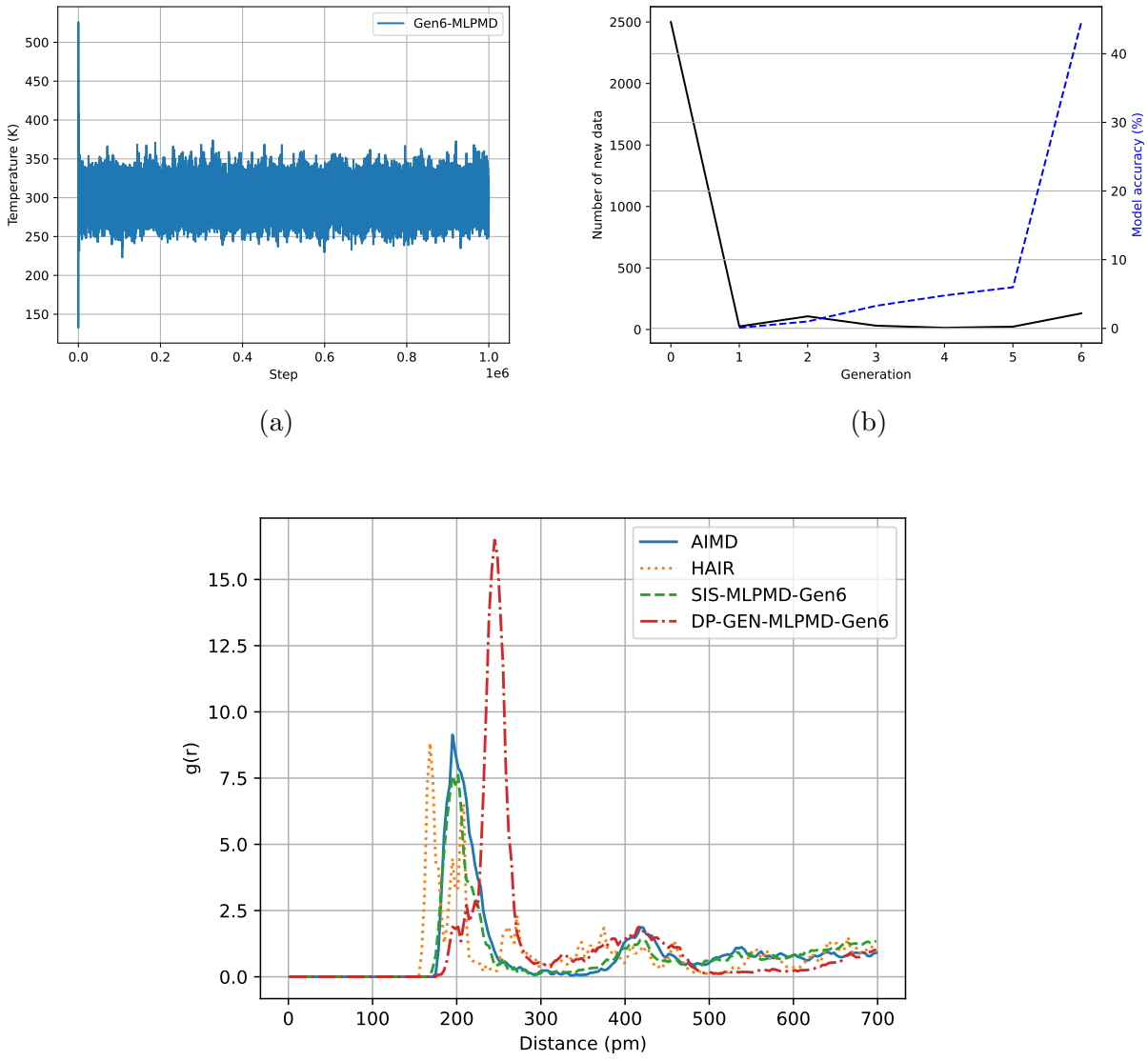

(a) (b)

(c)

Figure 3: (a) Temperature fluctuation in our 1 ns MLPMD simulation. (b) Number of new training data and model accuracy in each generation of DP-GEN. (c) Li-O (DOL) RDF comparison between HAIR, SIS-MLPMD and DP-GEN-MLPMD simulation trajectory, with AIMD result as the reference, see detailed data in Tab.S17.

For accuracy comparison, as it is not practical to use HAIR for energy/force test, here we choose to use RDF prediction (Li-O (DOL)) to measure model accuracy. As we need AIMD result as the ground truth for the comparison and AIMD simulation is impractical for long-time simulation, we extract a short trajectory (2.5 ps to 8 ps) for RDF calculation.

We choose this time range as we did not use DFT training data from it. For HAIR, the simulation consists 0.5 ps AIMD and 5 ps ReaxFF-MD and the merged trajectory is used to calculate RDF. For SIS-MLPMD simulation, we directly used the trained model in Figure 3a. RDF results in Figure 3c suggest that our method gives RDF generally more consistent with AIMD reference, and HAIR produces two unphysical RDF peaks at around 200 pm. Note that unlike HAIR, our model only used DFT data for MLP training while did not use them for the RDF calculation, so our result could be further improved by running additional generations of SIS-MLPMD to further improve model quality, or combining short AIMD with long MLPMD while keeping a satisfied AR.

For a fair comparison between SIS and DP-GEN, we use Gen6 model of both sampling methods, i.e., MLPs after 6 iterations of adding new training data, see Figure 1a and Ref.[29] Note SIS and DP-GEN start from the same initial training data, i.e., first 2.5 ps AIMD of electrolyte solution, so their only difference is sampling strategy. After 6 iterations, our SIS method collects DFT data of 17500 configurations (i.e., 17.5 ps AIMD) of electrolyte solution while DP-GEN collects only 2831 configurations (see black solid line in Figure 3b). However, this does not suggest DP-GEN gives better sampling efficiency but poor sampling sufficiency as its model accuracy is only < 50 % (see the blue dashed line in Figure 3b), far from the convergence threshold of DP-GEN.[29] As a consequence, the unsatisfied model accuracy gives the DP-GEN-MLPMD-Gen6 RDF result in Figure 3c, which shows poor agreement with the AIMD reference. The root for this is that AL based sampling methods are strongly dependent on the diversity of initial training data, so various data augmentation methods are usually necessary, e.g., perturbing DFT-relaxed structures, collecting DFT labelled data from MD simulations with different temperature, pressure, unit cell, thermodynamic ensemble, etc, see Ref.[32,55,56] Without these data augmentation, the model evolution becomes slow (see Model accuracy in Figure 3b). As a contrast, our SIS method is less dependent on the diversity of initial training data. Although DP-GEN labels much less DFT data after 6 generations, this is meaningless if the model accuracy is low. Considering multiple MLPs (default 4 for

DP-GEN, so 24 MLP training for 6 iterations) need to be trained in each generation for AL-based sampling, the total computational cost is not necessarily smaller than that required by our SIS-MLPMD method.

3.4. Underlying instability consistency

As mentioned in the previous section, the main difference between DP-GEN and our SIS sampling strategy is that DP-GEN and other similar AL-based sampling methods needs to train multiple MLPs (usually 4 or even more) in each iteration for uncertainty estimation.[29,31] As a result, though these methods usually reduce the number of needed DFT training data and associated computational costs, this is realized by adding computational costs of MLP training, especially when multiple GPU are not available. As a contrast, our method just train one MLP but running multiple MLPMD.

To test whether training multiple MLPs is really necessary or not, we perform an experiment by training two MLPs with the same training data but different seed numbers (10 and 24) in MLP, see Figure 4a. After running their long-time MLPMD simulation, we spot their t_{cp}. However we only use t_{cp1} information here as the indicator to sample new training data. The simulation with refined MLP suggests that not only t_{cp1} itself is fixed by introducing training data around t_{cp1}, t_{cp0} in MLP0 is resolved as well. This observation means that the information in multiple MLPs, which is frequently used in AL based sampling, could be redundancy and add unnecessary costs.

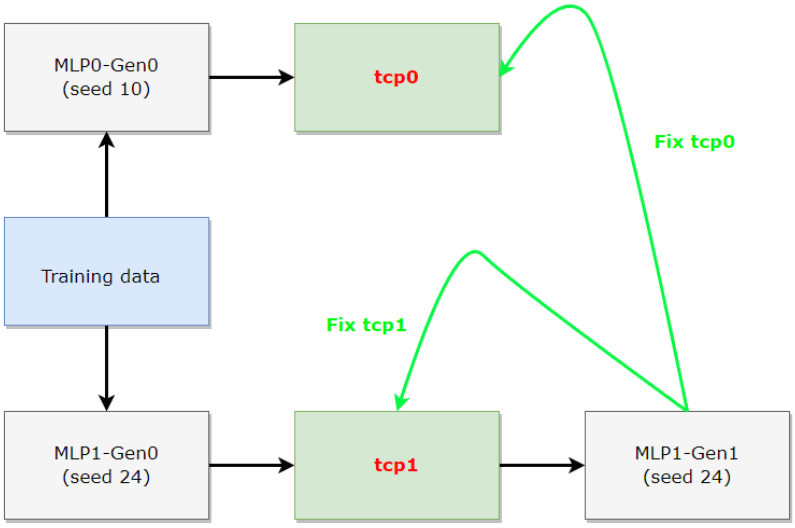

(a) Underlying instability consistency between different MLPs

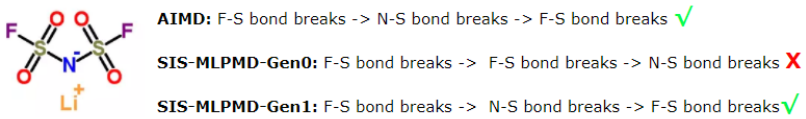

(b) Underlying instability consistency between temperature and reaction mechanism, see details in Fig.S9 and Fig.S10.

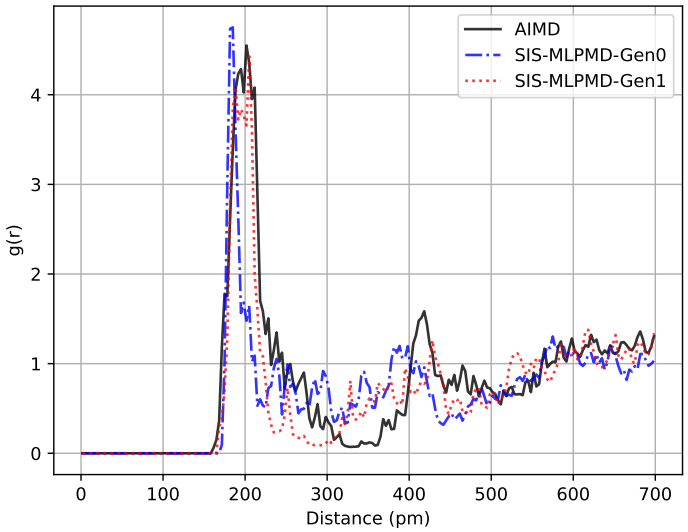

(c) Underlying instability consistency between temperature and RDF (Li-O(DOL), 0 to 2.5 ps)

Figure 4: Evidence for *underlying instability consistency* across different MLPs and properties.

Besides, many sampling methods to develop MLP rely on monitoring multiple properties

such as inter-atomic distances and RDF together in one loss function.[33,56] Here we intend to prove it is less necessary than previously reported as the underlying instability consistency guarantees model improvement transferable between properties (see Figure 4b and Figure 4c).

Bond breaking sequence of Lithium salt and solvent molecules is one crucial factor in studying SEI formation, as different bond breaking mechanism gives distinctly different SEI components and structures.[5] This stands for the heart for electrolyte engineering of batteries. As mentioned in Section 3.1, the AIMD ground-truth of bond breaking sequence of LiFSI is that one F-S bond breaks first, followed by N-S bond breaking, and finally the other F-S bond breaks, as illustrated in Fig.S2. However, our SIS-MLPMD-Gen0 simulation gives a wrong prediction where both two F-S bond breaks before the N-S bond breaking, see the reaction process in Fig.S9. After only one additional generation (i.e., SIS-MLPMD-Gen1 in Figure 4b), the reaction mechanism becomes correct, see Fig.S10. Additionally, the results in Figure 4c also suggests the RDF agreement with AIMD reference is improved after one additional generation of SIS-MLPMD. Note none of their information of reaction mechanism and RDF is explicitly used in our sampling as we use temperature instability information as the only sampling indicator. So we can conclude the underlying instability consistency is true across different properties. Using multiple properties (e.g., temperature, reaction mechanism, and RDF) together as sampling indicators could give redundant information.

Besides HAIR and DP-GEN, here we also highlight the difference of our SIS-MLPMD method compared with some other relevant works. For a similar target application scenario of electrolyte solution (though without reactions), Dajnowicz and co-workers developed a sampling strategy using both uncertainty estimation and the so-called *spurious reaction*.[56] However, the definition of *spurious reaction* is unclear and may rely on monitoring multiple properties in the simulation such as interatomic distance and RDF like that in the work of Fu and co-workers.[33] Additionally, one point worth to be highlighted particularly is that our implementation of *learning without forgetting* mechanism by using a decreased initial learning

rate.[37] Though the strategy is simple and more complicated methods to solve *catastrophic forgetting* issues exist in other tasks in computer vision and natural language processing,[57,58] their use in MLP is currently less uncovered.[29,56] Results in Tab.S1-S3 suggest this strategy is effective and non-trivial. Similarly for modeling reactions (though not battery systems), some works employed enhanced sampling methods to aid the sampling of training data,[25,59] which is not practical for modelling SEI formation because of the complex reaction network hinders the design of simple collective variables. However, combining our SIS-MLPMD method with other advanced sampling and generative models could be a direction forward to develop general reactive MLPs beyond CHNO species.[27,33] Magar and Farimani recently proposed two sampling strategies by re-distributing data iteratively (transfering data from test set to training set) leveraging the data point with largest test error and its similar points,[60] however, the recent work of Fu and co-workers suggests only energy or force error is not sufficient for sampling,[33] besides, the current implementation of their method requires building the whole database (e.g., 18928 data points for perovskites) in the first place, while no new data is added into this database (i.e., fixed 18928 data points) through the iterations, so it inherently has higher requirement with the diversity and size of the database.

3.5. Long-time MLPMD simulation of interfaces

Here we report long-time simulation of both 1 M and 10 M interfaces of Li|LiFSI/DOL. For both systems, the time length of MLPMD simulation reaches over 1 ns after 3 iterations of SIS-MLPMD. For 1 M interface, using just 16.5 ps AIMD training data gives stable MLPMD over 10 ns, which gives AR as over 606. While for 10 M interface, though the system is complicated, using 21 ps AIMD training data gives stable MLPMD over 3 ns, which gives its AR as over 142. The temperature of both systems is well located around our target value, 300 K, see Figure 5a and Figure 5b.

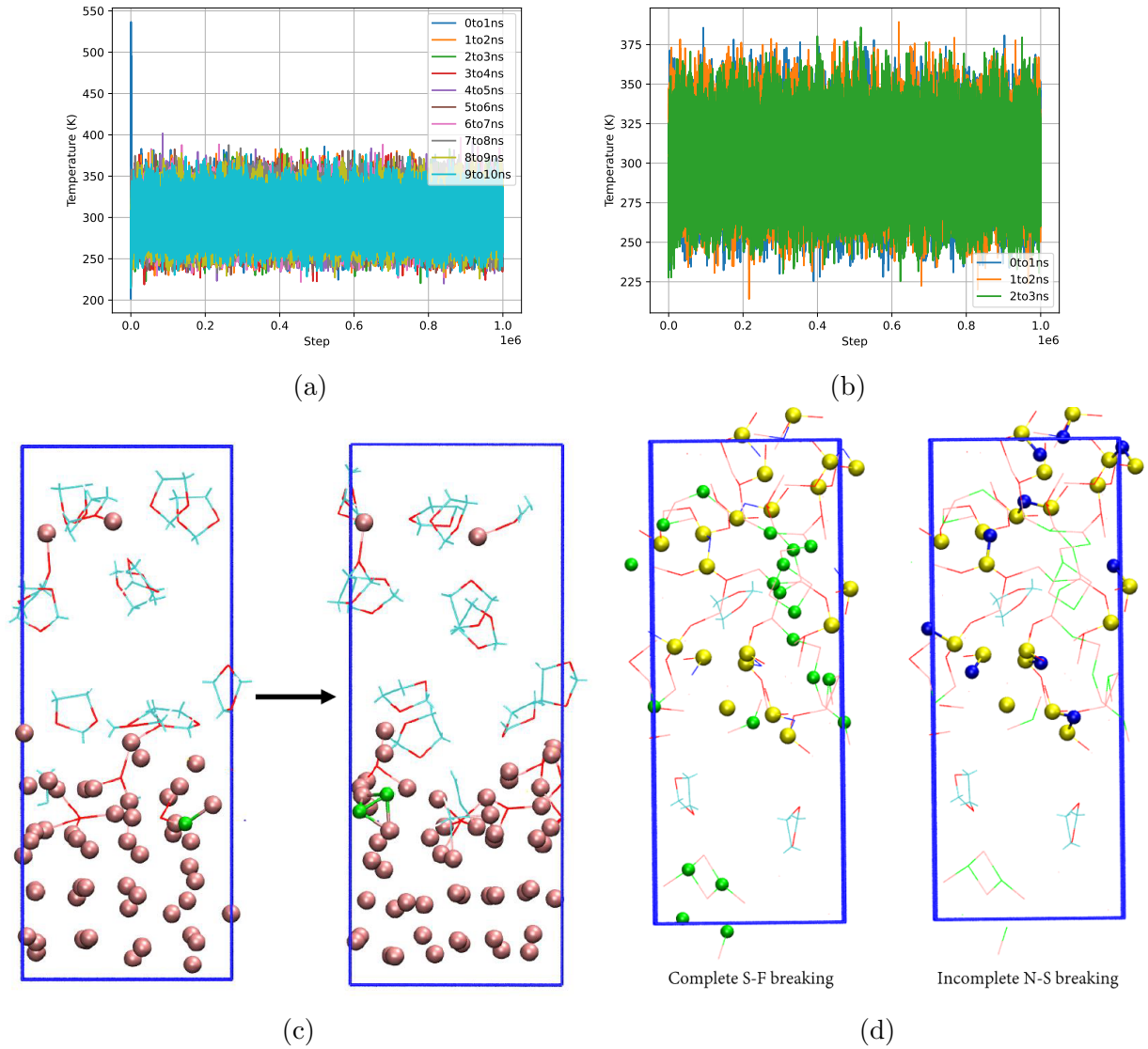

Figure 5: Good temperature stability of (a) 1M and (b) 10 M interface systems. (c) Ion aggregations of LiF to form Li_2F_2. (d) Complete S-F breaking and incomplete N-S breaking for 10 M interface system. For clarity, we only use CPK drawing style for relevant atoms in VMD.

Our MLPMD trajectories can reproduce some well-known SEI components including LiF, Li_2O, LiOH, LiS. More interestingly, ionic aggregation of LiF is observed in our long MLPMD simulation of 1M Li|LiFSI/DOL interface system (see Figure 5c), though it is not found in our AIMD training data. A possible reason why we did not observe it in AIMD simulation is that AIMD sampling configurations (those in the 16.5 ps AIMD trajectories)

and that in ionic aggregation region give similar MLP, while they are far in the configuration space. This phenomenon is physical according to previous works with accurate post-HF methods and electrochemical impedance spectroscopy.[61,62] Jones and co-workers concluded that the experimental molar conductivity Λ can be fitted by taking into account higher ion aggregations.[62] Considering LiF is one determining component in studying SEI while current understanding of it is limited[1] and the importance of Li_2F_2 has not been well recognized,[63,64] the properties of Li_2F_2 and even larger ion aggregation structures deserve more investigations in the future, which remains true even for low-concentration battery systems. For high-concentration system (see Figure 5d), in our MLPMD simulation we observe complete S-F breaking, incomplete N-S breaking and no DOL decomposition, which agrees well with the central finding in Ref.[5] for the mechanism of electrolyte concentration effects on SEI. This further validates the accuracy of our method while our simulation reaches the conclusion requiring much less ($< 20\%$ of that in HAIR, see Section 3.3) computational costs for AIMD.

4. Conclusions

This work presents a method (SIS-MLPMD) for efficiently sampling training data in developing MLP and associated MD simulations. The method leverages physics information (temperature instability information) as the sampling indicator. The efficiency and accuracy of our method is justified by comparing it with previous sophisticated physics-based and data-driven models, HAIR and DP-GEN. Our sampling strategy is found less dependent on the diversity of initial training data. With SIS-MLPMD, we study the bond breaking sequence of LiFSI in DOL solvent and the associated mechanism in the formation of SEI in LMB. Some crucial while frequently ignored factors are highlighted. Our study suggests using larger R_{cut} values does not guarantee higher accuracy, especially for interface systems and low-concentration electrolyte solution. We found using bulk configurations and avoid fixing atoms are crucial to develop MLP for interfaces. We propose the concept of underlying

instability consistency by showing MLP improvement can be transferable between different MLPs and properties. Our long-time MLPMD simulation reveals the incomplete N-S breaking in high-concentration systems, which echoes previous works with HAIR simulation.[5] Finally, our long-time MLPMD simulation suggests ion aggregation of LiF deserves further investigations for better understanding of SEI. Our work will be useful for future studies on reaction dynamics in interfaces, e.g., the long-time simulation of Lithium crystallization process at solid interfaces.[65]

Based on our work, future research can be developed along different directions: (1) The sampling efficiency could be further improved by using uncorrelated configurations from AIMD trajectories. The uncorrelated configurations could be chosen using a fixed time step or other techniques such as entropy maximization[66] and Minimum-Redundancy-Maximum-Relevance (MRMR).[67] (2) Our method can be combined with physical methods, AL based sampling techniques and deep generative models in different fashions, e.g., SIS-MLPMD works as the data augmentation strategy to build a diverse initial dataset, which is expected to significantly accelerate AL based sampling[29,31] and to refine molecule/conformation generations.[34] Additionally, short AIMD and long MLPMD can be combined in a similar way of HAIR.[5] Conformation/configuration generation module can be used to generate initial training data with high diversity, similar with the implementation in Uni-Mol+.[68] (3) Transforming MD simulation and associated data sampling problems into time sequence problems.[69,70] (4) Incorporating field effects in MLP for modelling charged interfaces under external potential.[22]

Acknowledgement

We acknowledge the helpful suggestions from Prof. Ruijuan Xiao (Institute of Physics, Chinese Academy of Sciences). We thank Prof. Tao Cheng (Soochow University) and Dr. Yue Liu (Soochow University) for sharing files for their HAIR simulation. We thank

DeepModeling community for helpful discussions with using DeepMD-kit and DP-GEN.

Supporting Information Available

More details in SIS-MLPMD workflow including training data generation, training and test of MLP. More details about the bond breaking sequence of LiFSI in DOL. Hyper-parameters effects and detailed results of the tests on R_{cut}, bulk configurations and fixing atoms. More detailed results for the comparison between SIS-MLPMD, HAIR and DP-GEN.

References

(1) Meng, Y. S.; Srinivasan, V.; Xu, K. Designing better electrolytes. *Science* **2022**, *378*, eabq3750.

(2) Diddens, D.; Appiah, W. A.; Mabrouk, Y.; Heuer, A.; Vegge, T.; Bhowmik, A. Modeling the Solid Electrolyte Interphase: Machine Learning as a Game Changer? *Advanced Materials Interfaces* **2022**, *9*, 2101734.

(3) Kim, J.-S.; Yoon, G.; Kim, S.; Sugata, S.; Yashiro, N.; Suzuki, S.; Lee, M.-J.; Kim, R.; Badding, M.; Song, Z., et al. Surface engineering of inorganic solid-state electrolytes via interlayers strategy for developing long-cycling quasi-all-solid-state lithium batteries. *Nature Communications* **2023**, *14*, 782.

(4) Peled, E.; Menkin, S. SEI: past, present and future. *Journal of The Electrochemical Society* **2017**, *164*, A1703.

(5) Liu, Y.; Sun, Q.; Yu, P.; Wu, Y.; Xu, L.; Yang, H.; Xie, M.; Cheng, T.; Goddard III, W. A. Effects of high and low salt concentrations in electrolytes at lithium–metal anode surfaces using DFT-ReaxFF hybrid molecular dynamics method. *The Journal of Physical Chemistry Letters* **2021**, *12*, 2922–2929.

(6) Yu, P.; Sun, Q.; Liu, Y.; Ma, B.; Yang, H.; Xie, M.; Cheng, T. Multiscale Simulation of Solid Electrolyte Interface Formation in Fluorinated Diluted Electrolytes with Lithium Anodes. *ACS Applied Materials & Interfaces* **2022**, *14*, 7972–7979.

(7) Yu, Z.; Rudnicki, P. E.; Zhang, Z.; Huang, Z.; Celik, H.; Oyakhire, S. T.; Chen, Y.; Kong, X.; Kim, S. C.; Xiao, X., et al. Rational solvent molecule tuning for high-performance lithium metal battery electrolytes. *Nature Energy* **2022**, *7*, 94–106.

(8) Liu, G.-X.; Tian, J.-X.; Wan, J.; Li, Y.; Shen, Z.-Z.; Chen, W.-P.; Zhao, Y.; Wang, F.; Liu, B.; Xin, S., et al. Revealing the High Salt Concentration Manipulated Evolution Mechanism on the Lithium Anode in Quasi-Solid-State Lithium-Sulfur Batteries. *Angewandte Chemie International Edition* **2022**, *61*, e202212744.

(9) Chen, X.; Zhang, X.-Q.; Li, H.-R.; Zhang, Q. Cation- solvent, cation- anion, and solvent- solvent interactions with electrolyte solvation in lithium batteries. *Batteries & Supercaps* **2019**, *2*, 128–131.

(10) Yao, N.; Chen, X.; Fu, Z.-H.; Zhang, Q. Applying classical, ab initio, and machine-learning molecular dynamics simulations to the liquid electrolyte for rechargeable batteries. *Chemical Reviews* **2022**, *122*, 10970–11021.

(11) Van Duin, A. C.; Dasgupta, S.; Lorant, F.; Goddard, W. A. ReaxFF: a reactive force field for hydrocarbons. *The Journal of Physical Chemistry A* **2001**, *105*, 9396–9409.

(12) Bannwarth, C.; Ehlert, S.; Grimme, S. GFN2-xTB—An accurate and broadly parametrized self-consistent tight-binding quantum chemical method with multipole electrostatics and density-dependent dispersion contributions. *Journal of chemical theory and computation* **2019**, *15*, 1652–1671.

(13) Unke, O. T.; Chmiela, S.; Sauceda, H. E.; Gastegger, M.; Poltavsky, I.; Schutt, K. T.; Tkatchenko, A.; Muller, K.-R. Machine learning force fields. *Chemical Reviews* **2021**, *121*, 10142–10186.

(14) Zhang, L.; Han, J.; Wang, H.; Car, R.; Weinan, E. Deep potential molecular dynamics: a scalable model with the accuracy of quantum mechanics. *Physical review letters* **2018**, *120*, 143001.

(15) Jiao, J.; Lai, G.; Zhao, L.; Lu, J.; Li, Q.; Xu, X.; Jiang, Y.; He, Y.-B.; Ouyang, C.; Pan, F., et al. Self-healing mechanism of lithium in lithium metal. *Advanced Science* **2022**, *9*, 2105574.

(16) Batzner, S.; Musaelian, A.; Sun, L.; Geiger, M.; Mailoa, J. P.; Kornbluth, M.; Molinari, N.; Smidt, T. E.; Kozinsky, B. E (3)-equivariant graph neural networks for data-efficient and accurate interatomic potentials. *Nature communications* **2022**, *13*, 2453.

(17) Wang, F.; Sun, Y.; Cheng, J. Switching of Redox Levels Leads to High Reductive Stability in Water-in-Salt Electrolytes. *Journal of the American Chemical Society* **2023**, *145*, 4056–4064.

(18) Dufils, T.; Schran, C.; Chen, J.; Geim, A. K.; Fumagalli, L.; Michaelides, A. Understanding the anomalously low dielectric constant of confined water: an ab initio study. *arXiv preprint arXiv:2211.14035* **2022**,

(19) Eckhoff, M.; Behler, J. Insights into lithium manganese oxide–water interfaces using machine learning potentials. *The Journal of Chemical Physics* **2021**, *155*, 244703.

(20) Frank, T.; Unke, O.; Müller, K.-R. So3krates: Equivariant attention for interactions on arbitrary length-scales in molecular systems. *Advances in Neural Information Processing Systems* **2022**, *35*, 29400–29413.

(21) Zhai, Y.; Caruso, A.; Bore, S. L.; Luo, Z.; Paesani, F. A "short blanket" dilemma for a state-of-the-art neural network potential for water: Reproducing experimental properties or the physics of the underlying many-body interactions? *The Journal of Chemical Physics* **2023**, *158*, 084111.

(22) Gastegger, M.; Schütt, K. T.; Müller, K.-R. Machine learning of solvent effects on molecular spectra and reactions. *Chemical science* **2021**, *12*, 11473–11483.

(23) Vogel, Y. B.; Evans, C. W.; Belotti, M.; Xu, L.; Russell, I. C.; Yu, L.-J.; Fung, A. K.; Hill, N. S.; Darwish, N.; Gonçales, V. R., et al. The corona of a surface bubble promotes electrochemical reactions. *Nature Communications* **2020**, *11*, 6323.

(24) Zeng, J.; Zhang, L.; Wang, H.; Zhu, T. Exploring the chemical space of linear alkane pyrolysis via deep potential generator. *Energy & fuels* **2020**, *35*, 762–769.

(25) Yang, M.; Bonati, L.; Polino, D.; Parrinello, M. Using metadynamics to build neural network potentials for reactive events: the case of urea decomposition in water. *Catalysis Today* **2022**, *387*, 143–149.

(26) Blau, S. M.; Patel, H. D.; Spotte-Smith, E. W. C.; Xie, X.; Dwaraknath, S.; Persson, K. A. A chemically consistent graph architecture for massive reaction networks applied to solid-electrolyte interphase formation. *Chemical science* **2021**, *12*, 4931–4939.

(27) Zhang, S.; Makoś, M.; Jadrich, R.; Kraka, E.; Barros, K.; Nebgen, B.; Tretiak, S.; Isayev, O.; Lubbers, N.; Messerly, R., et al. Exploring the frontiers of chemistry with a general reactive machine learning potential. **2022**,

(28) Wen, Y.; Li, Z.; Xiang, Y.; Reker, D. Improving Molecular Machine Learning Through Adaptive Subsampling with Active Learning. *Digital Discovery* **2023**,

(29) Zhang, Y.; Wang, H.; Chen, W.; Zeng, J.; Zhang, L.; Wang, H.; Weinan, E. DP-GEN: A concurrent learning platform for the generation of reliable deep learning based potential energy models. *Computer Physics Communications* **2020**, *253*, 107206.

(30) Carrete, J.; Montes-Campos, H.; Wanzenböck, R.; Heid, E.; Madsen, G. K. Deep ensembles vs committees for uncertainty estimation in neural-network force fields: Com-

parison and application to active learning. *The Journal of Chemical Physics* **2023**, *158*.

(31) Kulichenko, M.; Barros, K.; Lubbers, N.; Li, Y. W.; Messerly, R.; Tretiak, S.; Smith, J. S.; Nebgen, B. Uncertainty-driven dynamics for active learning of interatomic potentials. *Nature Computational Science* **2023**, 1–10.

(32) Huang, J.; Zhang, L.; Wang, H.; Zhao, J.; Cheng, J.; E, W. Deep potential generation scheme and simulation protocol for the Li10GeP2S12-type superionic conductors. *The Journal of Chemical Physics* **2021**, *154*, 094703.

(33) Fu, X.; Wu, Z.; Wang, W.; Xie, T.; Keten, S.; Gomez-Bombarelli, R.; Jaakkola, T. Forces are not enough: Benchmark and critical evaluation for machine learning force fields with molecular simulations. *arXiv preprint arXiv:2210.07237* **2022**,

(34) Wu, F.; Li, S. Z. DIFFMD: A Geometric Diffusion Model for Molecular Dynamics Simulations. **2023**,

(35) Kühne, T. D.; Iannuzzi, M.; Del Ben, M.; Rybkin, V. V.; Seewald, P.; Stein, F.; Laino, T.; Khaliullin, R. Z.; Schütt, O.; Schiffmann, F., et al. CP2K: An electronic structure and molecular dynamics software package-Quickstep: Efficient and accurate electronic structure calculations. *The Journal of Chemical Physics* **2020**, *152*, 194103.

(36) Wang, H.; Zhang, L.; Han, J.; Weinan, E. DeePMD-kit: A deep learning package for many-body potential energy representation and molecular dynamics. *Computer Physics Communications* **2018**, *228*, 178–184.

(37) Li, Z.; Hoiem, D. Learning without forgetting. *IEEE transactions on pattern analysis and machine intelligence* **2017**, *40*, 2935–2947.

(38) Thompson, A. P.; Aktulga, H. M.; Berger, R.; Bolintineanu, D. S.; Brown, W. M.; Crozier, P. S.; in't Veld, P. J.; Kohlmeyer, A.; Moore, S. G.; Nguyen, T. D., et al.

LAMMPS-a flexible simulation tool for particle-based materials modeling at the atomic, meso, and continuum scales. *Computer Physics Communications* **2022**, *271*, 108171.

(39) Camacho-Forero, L. E.; Smith, T. W.; Balbuena, P. B. Effects of high and low salt concentration in electrolytes at lithium–metal anode surfaces. *The Journal of Physical Chemistry C* **2017**, *121*, 182–194.

(40) Sodeyama, K.; Yamada, Y.; Aikawa, K.; Yamada, A.; Tateyama, Y. Sacrificial anion reduction mechanism for electrochemical stability improvement in highly concentrated Li-salt electrolyte. *The Journal of Physical Chemistry C* **2014**, *118*, 14091–14097.

(41) Wang, A.; Kadam, S.; Li, H.; Shi, S.; Qi, Y. Review on modeling of the anode solid electrolyte interphase (SEI) for lithium-ion batteries. *npj Computational Materials* **2018**, *4*, 15.

(42) Chen, C.; Ong, S. P. A universal graph deep learning interatomic potential for the periodic table. *Nature Computational Science* **2022**, *2*, 718–728.

(43) Zhuang, Y.-B.; Bi, R.-H.; Cheng, J. Resolving the odd–even oscillation of water dissociation at rutile TiO2 (110)–water interface by machine learning accelerated molecular dynamics. *The Journal of Chemical Physics* **2022**, *157*, 164701.

(44) Wu, J.; Yang, J.; Ma, L.; Zhang, L.; Liu, S. Modular developing deep potential for complex solid solutions. *arXiv preprint arXiv:2301.06298* **2023**,

(45) Elliott, S. D.; Greer, J. C. Simulating the atomic layer deposition of alumina from first principles. *Journal of Materials Chemistry* **2004**, *14*, 3246–3250.

(46) Hameeuw, K.; Cantele, G.; Ninno, D.; Trani, F.; Iadonisi, G. The rutile TiO 2 (110) surface: Obtaining converged structural properties from first-principles calculations. *The Journal of chemical physics* **2006**, *124*, 024708.

(47) Manna, S.; Loeffler, T. D.; Batra, R.; Banik, S.; Chan, H.; Varughese, B.; Sasikumar, K.; Sternberg, M.; Peterka, T.; Cherukara, M. J., et al. Learning in continuous action space for developing high dimensional potential energy models. *Nature communications* **2022**, *13*, 368.

(48) Hu, T.; Tian, J.; Dai, F.; Wang, X.; Wen, R.; Xu, S. Impact of the Local Environment on Li Ion Transport in Inorganic Components of Solid Electrolyte Interphases. *Journal of the American Chemical Society* **2022**,

(49) Batatia, I.; Kovacs, D. P.; Simm, G.; Ortner, C.; Csányi, G. MACE: Higher order equivariant message passing neural networks for fast and accurate force fields. *Advances in Neural Information Processing Systems* **2022**, *35*, 11423–11436.

(50) Li, Q.; Ouyang, Y.; Lu, S.; Bai, X.; Zhang, Y.; Shi, L.; Ling, C.; Wang, J. Perspective on theoretical methods and modeling relating to electro-catalysis processes. *Chemical Communications* **2020**, *56*, 9937–9949.

(51) Jirkovsky, J. S.; Panas, I.; Ahlberg, E.; Halasa, M.; Romani, S.; Schiffrin, D. J. Single atom hot-spots at Au–Pd nanoalloys for electrocatalytic H2O2 production. *Journal of the American Chemical Society* **2011**, *133*, 19432–19441.

(52) Fang, W.; Jiang, H.; Zheng, Y.; Zheng, H.; Liang, X.; Sun, Y.; Chen, C.; Xiang, H. A bilayer interface formed in high concentration electrolyte with SbF3 additive for long-cycle and high-rate sodium metal battery. *Journal of Power Sources* **2020**, *455*, 227956.

(53) Wang, Y.; Jiang, R.; Liu, Y.; Zheng, H.; Fang, W.; Liang, X.; Sun, Y.; Zhou, R.; Xiang, H. Enhanced Sodium Metal/Electrolyte Interface by a Localized High-Concentration Electrolyte for Sodium Metal Batteries: First-Principles Calculations and Experimental Studies. *ACS Applied Energy Materials* **2021**, *4*, 7376–7384.

(54) Huang, J.; Yan, T.; Tao, M.; Zhang, W.; Li, W.; Zheng, G.; Du, L.; Cui, Z.; Wang, X.; Liao, S., et al. Localized high-concentration carbonate electrolyte creating functional in situ interfaces: Side reaction inhibition for lithium sulfur batteries. *Journal of Power Sources* **2023**, *563*, 232783.

(55) Xu, T.; Li, X.; Wang, Y.; Tang, Z. Development of Deep Potentials of Molten MgCl2–NaCl and MgCl2–KCl Salts Driven by Machine Learning. *ACS Applied Materials & Interfaces* **2023**, *15*, 14184–14195.

(56) Dajnowicz, S.; Agarwal, G.; Stevenson, J. M.; Jacobson, L. D.; Ramezanghorbani, F.; Leswing, K.; Friesner, R. A.; Halls, M. D.; Abel, R. High-dimensional neural network potential for liquid electrolyte simulations. *The Journal of Physical Chemistry B* **2022**, *126*, 6271–6280.

(57) Kirkpatrick, J.; Pascanu, R.; Rabinowitz, N.; Veness, J.; Desjardins, G.; Rusu, A. A.; Milan, K.; Quan, J.; Ramalho, T.; Grabska-Barwinska, A., et al. Overcoming catastrophic forgetting in neural networks. *Proceedings of the national academy of sciences* **2017**, *114*, 3521–3526.

(58) Ramasesh, V. V.; Lewkowycz, A.; Dyer, E. Effect of scale on catastrophic forgetting in neural networks. International Conference on Learning Representations. 2022.

(59) Vandenhaute, S.; Cools-Ceuppens, M.; DeKeyser, S.; Verstraelen, T.; Van Speybroeck, V. Machine learning potentials for metal-organic frameworks using an incremental learning approach. *npj Computational Materials* **2023**, *9*, 19.

(60) Magar, R.; Farimani, A. B. Learning from mistakes: Sampling strategies to efficiently train machine learning models for material property prediction. *Computational Materials Science* **2023**, *224*, 112167.

(61) Srivastava, A. K.; Misra, N. Can Li2F2 cluster be formed by LiF2/Li2F–Li/F interactions? An ab initio investigation. *Molecular Simulation* **2015**, *41*, 1278–1282.

(62) Jones, J.; Anouti, M.; Caillon-Caravanier, M.; Willmann, P.; Lemordant, D. Lithium fluoride dissolution equilibria in cyclic alkylcarbonates and water. *Journal of Molecular Liquids* **2010**, *153*, 146–152.

(63) Tan, J.; Matz, J.; Dong, P.; Shen, J.; Ye, M. A growing appreciation for the role of LiF in the solid electrolyte interphase. *Advanced Energy Materials* **2021**, *11*, 2100046.

(64) Ren, Y.; Qi, Z.; Ma, X.; Yang, S.; Zhang, C.; Tan, X.; Liu, X. First-principles study of the effect of mechanical strength on ion transport in La-doped LiF-SEI on the Li (001) surface. *Materials Today Chemistry* **2021**, *20*, 100451.

(65) Yang, M.; Liu, Y.; Mo, Y. Lithium crystallization at solid interfaces. *Nature Communications* **2023**, *14*, 2986.

(66) Shewry, M. C.; Wynn, H. P. Maximum entropy sampling. *Journal of applied statistics* **1987**, *14*, 165–170.

(67) Ramírez-Gallego, S.; Lastra, I.; Martínez-Rego, D.; Bolón-Canedo, V.; Benítez, J. M.; Herrera, F.; Alonso-Betanzos, A. Fast-mRMR: Fast minimum redundancy maximum relevance algorithm for high-dimensional big data. *International Journal of Intelligent Systems* **2017**, *32*, 134–152.

(68) Lu, S.; Gao, Z.; He, D.; Zhang, L.; Ke, G. Highly Accurate Quantum Chemical Property Prediction with Uni-Mol+. *arXiv preprint arXiv:2303.16982* **2023**,

(69) Tsai, S.-T.; Kuo, E.-J.; Tiwary, P. Learning molecular dynamics with simple language model built upon long short-term memory neural network. *Nature communications* **2020**, *11*, 5115.

(70) Zeng, W.; Cao, S.; Huang, X.; Yao, Y. A note on learning rare events in molecular dynamics using lstm and transformer. *arXiv preprint arXiv:2107.06573* **2021**,

TOC Graphic